Effects of Rosin-Type Clarifying Agent on the Crystallization and Compatibility of Polypropylene and Low Density Polyethylene

Hui Wang, Chun-Cheng Li, Yu-Cai Ke, Dong Zhang, Zhen-Yi Li

CAS Key Laboratory of Engineering Plastics, Joint Laboratory of Polymer Science and Materials, Center for Molecular Science, Institute of Chemistry, The Chinese Academy of Sciences, Beijing 100080, People's Republic of China

ABSTRACT: In this article, the influence of rosin-type clarifying agent Nu-(K + Na) and low density polyethylene (LDPE) on the crystallization process of polypropylene (PP) from the melt state was studied by differential scanning calorimeter and polarization microscope, and the effect of rosin-type clarifying agent Nu-(K + Na) on the compatibility of PP and LDPE was also investigated by dynamic mechanical analysis and scanning electron microscope. It was found that Nu-(K + Na) decreased the fold surface energy and promoted the nucleation and crystallization of PP. With the cooperation of LDPE and Nu-(K + Na) in PP, the chain fold free energy of PP was further decreased substantially, the crystallization rate of PP was increased more markedly, and the spherulites of PP became much smaller and dispersed more uniformly. At the same time, Nu-(K + Na) improved the compatibility of PP and LDPE, and the LDPE was dispersed in PP more uniformly. Thus, the light scattering originating from the spherulites of PP and the LDPE disperse phase was reduced to great extent, and the transparency of PP was improved evidently. © 2005 Wiley Periodicals, Inc. J Appl Polym Sci 99: 1568–1575, 2006

Key words: poly(propylene); polyethylene; crystallization; compatibility

INTRODUCTION

In the last few years, a new kind of rosin-type clarifying agent for polypropylene (PP), which can greatly improve the transparency of PP, was reported in several patents.[1–3] Rather than the conventional clarifying agents widely used before, these clarifying agents had some advantages, such as low production cost, high nucleating efficiency, and without irritative odor.[1–3] In our earlier works,[4–6] the effects of rosin-type clarifying agent on PP crystallization had been studied, and it was found that rosin-type clarifying agent accelerated the overall crystallization rate of PP, diminished the size of spherulites, and improved the transparency of PP to a certain extent. Further research found that the nucleating efficiency of rosin-type nucleating agent could be improved greatly when a small amount of low density polyethylene (LDPE) (3%) was added to PP.[7] The cooperative effect of LDPE and rosin-type clarifying agent made the crystallization rate of PP increase greatly, the spherulites of PP became much smaller and dispersed more uniformly, and the transparency of PP was further improved

evidently. To get better transparency of PP in former works, the content of rosin-type clarifying agent in PP must be above 5%, which is much higher than the loading of other clarifying agents, such as dibenzylidene sorbitol (DBS).[8]

To further decrease the loading of rosin-type clarifying agent in PP, a new kind of rosin-type clarifying agent for PP, the cocrystal of dehydroabietic acid, potassium dehydroabietate, and sodium dehydroabietate (Nu-(K + Na)), was prepared.[9] In this study, it was found that when 3% LDPE and 0.3% Nu-(K + Na) was added to PP at the same time, the transparency of PP improved substantially. PP/LDPE blends, especially their compatibility and morphology, have been studied extensively,[10–15] but only a few studies have been reported on the effects of clarifying agent on the crystallization and compatibility of PP and LDPE. In this article, the effects of rosin-type clarifying agent on the crystallization and compatibility of PP and LDPE were studied detailedly. The crystal structure of PP was also investigated.

EXPERIMENTAL

Materials

Isotactic PP (grade F401, melt index 2.5 g/10 min) and LDPE (grade 1C7A, melt index 7 g/10 min) were supplied by Beijng Yansan Petroleum and Chemical
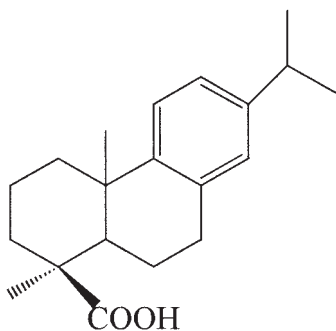
Figure 1 Structure of dehydroabietic acid.

Corp (Beijing, China). Dehydroabietic acid was separated from disproportionated rosin (Wuzhou Rosin Plant, Guangxi, China), according to the usual procedure,[16] and the structure of dehydroabietic acid was shown in Figure 1.

Preparation

Rosin-type cocrystal clarifying agent was prepared by the reaction of 1 mol dehydroabietic acid with 0.25 mol potassium hydroxide and 0.15 mol sodium dehydroabietate in ethanol, according to our previous research,[9] and then grinded into powder with a nominal particle size of 65 μm and marked as Nu-(K + Na).

PP, Nu-(K + Na), and LDPE were blended as follows: 100/0/0, 100/0/3, 100/0.3/0, 100/0.3/3, 100/0.3/5, 100/0.3/10, 100/0.3/15, and 100/0.3/20 (wt %), respectively. The composites were mixed in a Φ30 twin-screw extruder (SHJ-30, Light Industry Machinery Mold Factory, Shanghai, China). The nucleated PP samples were dried and then injection-molded into 1 mm thick sheet in an injection-molding machine (SZ-160/68 NB, Rubber Plastics Machinery Plant, Liuzhou, China) at 230°C.

Measurements

Haze measurement

Transparency was measured by a WGT-S hazemeter (Precision & Scientific Instrument Co. Ltd., Shanghai, China), according to National Standard Testing Methods GB 2410–80, and the lower the haze, the higher is the transparency.

Differential scanning calorimeter (DSC)

A Perkin–Elmer differential scanning calorimeter, DSC-7, interfaced with a BBC-Master computer *via* analogue to digital converter, was used to detect the thermal transition and to monitor the rate of heat flow from samples during crystallization. The instrument was calibrated by indium before the measurements.

Each sample (5± 2 mg) was placed in a DSC pan and rapidly heated at a rate of 80°C/min to 230°C for 10 min to remove all the memory of previous thermal and mechanical history.

To detect the crystallization temperatures of PP samples, this treatment was followed by cooling at a rate of 10°C/min to room temperature for complete crystallization.

In the experiments performed to study kinetics of isothermal crystallization, the samples were submitted to the same thermal treatment in melt state and then cooled at a rate of 200°C/min to the appropriate crystallizing temperature. The rate of heat flow during the development of crystalline phase against time was recorded up to vanishing thermal effect and analyzed according to the usual procedure to give the relative degree of crystallinity as a function of time.

Polarization microscope

Each PP sample (0.1 g) was placed on a hot-stage and melted at 230°C. Each PP sample was pressed between glass slides and cover slips and kept there for 10 min to remove all the memory of previous thermal and mechanical history, and then quickly transferred to another hot-stage and kept at a constant temperature of 130°C for 1 h. After that, they were quenched in liquid nitrogen. The thickness of PP samples was about 20 μm. The morphology of sperulites was observed by a polarization microscope (Leica MPS30, Germany).

Dynamic mechanical analysis

Dynamic mechanical analysis (DMA) measurements were performed with a Perkin–Elmer DMA-7. The instrument was calibrated by indium before the measurements. The experiments were carried out using the three-point-blending geometry over a temperature range of −150 to 200°C at a rate 5°C/min under nitrogen flow. All the samples were analyzed at a constant frequency of 1 Hz, a dynamic force 30 mN, and a static force 33 mN. The rectangular specimen dimensions were 15 × 2 × 2 mm^3.

Scanning electron microscope

The morphology of the fractured surfaces of the specimens was investigated with a scanning electron microscope (Hitachi S-530, Japan). The specimens were fractured after cooling in liquid nitrogen, and the fractured surfaces were sputter-coated with gold under argon atmosphere. The electron micrographs were taken using an acceleration voltage of 15.0 kV.

Nu-(K + Na) (%)	LDPE (%)					
	0	3	5	10	15	20
0	70	60	—	—	—	—
0.3	40	27	30	34	37	39

RESULTS AND DISCUSSION

Transparency of PP samples

Table I lists the haze values of the PP composites. The haze value of pure PP is 70%, and its transparency is the worst among all PP samples. The haze value of PP/Nu-(K + Na) (100:0.3) was decreased to 40%. When 0.3% Nu-(K + Na) and 3% LDPE were added to PP at the same time, the haze value of PP was further decreased to 27%. With more LDPE added, however, the haze values of the blends increased gradually. The PP/Nu-(K + Na)/LDPE (100:0.3:3) ternary blend exhibits the best transparency among all PP samples.

Transparency of the PP/Nu-(K + Na)/LDPE ternary blends was determined by two main factors: one was the spherulite size of PP particle, and the other was the size of the LDPE, which was related to its compatibility with PP. The effects of Nu-(K + Na) on the crystallization and compatibility of PP and LDPE were studied by the next experiments.

Nonisothermal crystallization of PP samples

Figure 2 shows DSC cooling curves of PP samples at a cooling rate of 10°C/min. An exothermic peak occurs at T_c = 111.7, 111.9, 121.4, and 126.8°C for PP/Nu-(K + Na)/LDPE (100/0/0), (100/0/3), (100/0.3/0), and (100/0.3/3), respectively. The dominative crystallization process of pure PP was homogeneous nucleation, the intense thermal motion of molecular chain segment made it difficult to form stable crystal nuclei at high temperature, and so its crystallization temperature was very low. The addition of 3% LDPE only slightly affected the T_c of PP. With 0.3% Nu-(K + Na) added, the T_c of PP/Nu-(K + Na) was increased 9.7°C compared with pure PP, this demonstrates that Nu-(K + Na) is an effective nucleating agent, and it increased the crystallization rate of PP obviously. When both 3% LDPE and 0.3% Nu-(K + Na) were added to PP, the increase in T_c of PP was 15.1°C compared with pure PP and its exothermic peak became much sharper than that of the others. This might be that the nucleating efficiency was increased evidently with the help of LDPE.

Isothermal crystallization of PP samples

Isothermal crystallization of polymers can be described by Avrami equation. The relative degree of crystallinity θ at time t is given by[17]

$$\theta = \frac{X_C(t)}{X_C(\infty)} = \int_0^t \frac{dH(t)}{dt}\,dt \bigg/ \int_0^\infty \frac{dH(t)}{dt}\,dt \qquad (1)$$

where $X_C(t)$ and $X_C(\infty)$ are the absolute degrees of crystallinity at time t and the completing crystallization time respectively, $dH(t)/dt$ is the rate of heat flow in the process of isothermal crystallization at time t. Time t was measured from the moment when the sample was cooled to the appropriate crystallization temperature. θ can also be obtained from the expression[17,18]

$$1 - \theta = \exp(-Kt^n) \qquad (2)$$

$$\ln(-\ln(1 - \theta)) = n \ln t + \ln K \qquad (3)$$

where n is Avrami exponent, which is determined by the mode of crystal nucleation and the crystal growth geometry in actual circumstance, and K is the rate constant, which is also a function of nucleation and growth of crystals. The plot of $\ln(-\ln(1-\theta))$ against $\ln t$ is a straight line, whose slope is n and its intercept on ordinate is $\ln K$.

When θ = 0.5 in formula (3), it gives out the data of crystallization half-time $t_{1/2}$, which is the time taken for 50% of the total crystallization to occur:

$$t_{1/2} = \left(\frac{\ln 2}{K}\right)^{\frac{1}{n}} \qquad (4)$$

The lowest temperature for isothermal crystallization was chosen to be above the highest temperature at which the LDPE was able to crystallize. Results of $t_{1/2}$, n, and K of PP samples are listed in Table II.
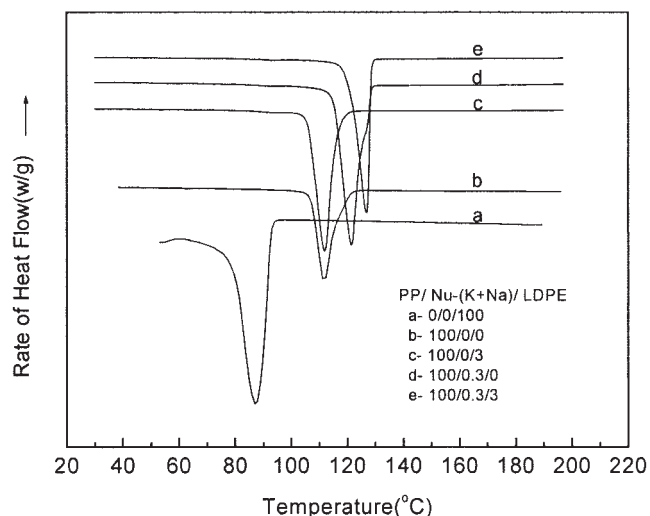

Figure 2 DSC curves of PP samples.

In the ideal state of heterogeneous nucleation of PP crystallization,[17] n should be exactly 3. In the actual process of crystal growth, the real circumstance cannot satisfy the ideal state that the Avrami equation supposes it to have. In addition, the practical measurement is determined by both the temperature and the thermal history of crystal growth.[18] In Table II, the rate constant K decreases as temperature increases. Temperatures at which isothermal crystallization was conducted are higher than that of the maximum rate of crystallization. Consequently, the higher the temperature of isothermal crystallization, the larger is the distance from the temperature of the maximum rate of crystallization and the lower is the rate of crystallization.

Figure 3 shows the crystallization half-time $t_{1/2}$ versus temperature. The rate of crystallization of polymers can be estimated by the crystallization half-time, when the crystallization temperature is the same. The samples that need a smaller $t_{1/2}$ have a faster rate of crystallization, if they crystallize at the same crystallization temperature. When T_c is 129°C, for PP/Nu-(K + Na)/LDPE (100/0/0), (100/0/3), (100/0.3/0), and (100/0.3/3), $t_{1/2}$ is 620, 605, 63, and 18 s, respectively. The addition of 3% LDPE only slightly affected the $t_{1/2}$ of PP. The $t_{1/2}$ of PP/Nu-(K + Na)/LDPE (100/0.3/0) was obviously reduced, this indicates that Nu-(K + Na) had good nucleating ability and increased the crystallization rate of PP. When both 0.3% Nu-(K + Na) and 3% LDPE were added, $t_{1/2}$ was further reduced. This also proves that the nucleating efficiency of Nu-(K + Na) was increased evidently with the help of LDPE.

In addition, we could obtain more information from the curves of the crystallization half-time versus crystallization temperature for PP samples (Fig. 3) As could be observed, within the range of crystallization
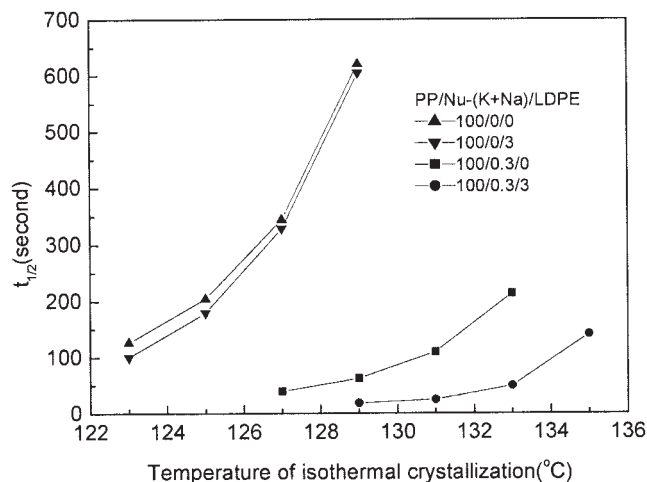
Figure 3 Curves of half-time of isothermal crystallization ($t_{1/2}$) versus temperature.

temperature studied, the two blends PP/Nu-(K + Na)/LDPE (100/0.3/0), (100/0.3/3), their crystallization rates ($t_{1/2}$) are not sensitive to temperature. This is helpful to erase the effect of different temperatures on the crystallization process and achieve a uniform structure and stable size products, especially in the thick parts. But the pure PP and PP blend without Nu-(K + Na) has the sensitive regions within the temperature range that had been studied here.

According to Hoffman nucleation theory of isothermal crystallization, the dependence of growth rate G on crystallization temperature T_c and on supercooling degree $\Delta T = T^0_m - T_c$ is described by the following equation:[19–22]

$$G = G_0 \exp\left(-\frac{U^*}{R(Tc - T\infty)}\right)\exp\left(-\frac{Kg}{fTc\Delta T}\right) \quad (4)$$

From Avrami equation, it can be shown that[23]

$$G \propto K^{1/n} \quad (5)$$

By combining eqs. (4) and (5), and after some rearrangement, it gives

$$\frac{U^*}{R(T_C - T_\infty)} + \frac{1}{n}\ln K \propto -\frac{Kg}{fTc\Delta T} \quad (6)$$

where

$$Kg = -\frac{4\sigma_{\sigma_e b_0 T^0_m}}{K_b \Delta H^0_m} \quad (7)$$

Here G_0 is the pre-exponential factor containing quantities not strongly dependent on the temperature; U^* is the activation energy of polymer segments trans-

TABLE II
Kinetic Parameters of the PP Blends

PP/Nu-(K + Na)/LDPE (Wt%)	T_c (°C)	K (s^{-n})	n	$t_{1/2}$ (s)
100/0/0	123	0.38×10^{-3}	1.51	126
	125	0.10×10^{-3}	1.62	2044
	127	0.16×10^{-4}	1.78	344
	129	0.20×10^{-4}	1.92	620
100/0/3	123	0.12×10^{-4}	2.28	101
	125	0.18×10^{-5}	2.38	179
	127	0.72×10^{-7}	2.67	328
	129	0.28×10^{-8}	2.92	605
100/0.3/0	127	0.50×10^{-2}	1.31	40
	129	0.13×10^{-2}	1.47	63
	131	0.32×10^{-3}	1.59	110
	133	0.71×10^{-5}	2.07	213
100/0.3/3	129	0.10×10^{-1}	1.32	18
	131	0.36×10^{-2}	1.58	25
	133	0.15×10^{-3}	2.06	48
	135	0.91×10^{-6}	2.62	141
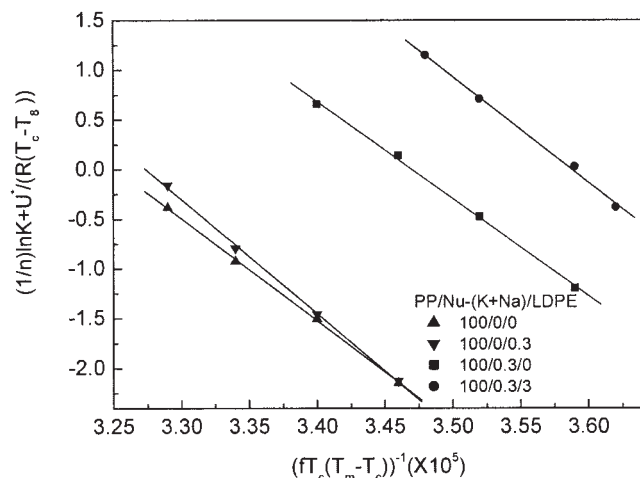
Figure 4 Curves of $1/n \ln K + U^*/(R(T_C - T_\infty))$ *versus* $(fTc\Delta T)^{-1}$.

porting to the crystal front through the subcooled melt; R is the gas constant; T_∞ is the theoretical temperature at which all motion associated with viscous flow ceases; b_0 is the monolayer thickness; σ and σ_e are the lateral and fold surface energies of the developing crystals in PP bulk respectively, T_c is the crystallization temperature; T^0_m is the equilibrium melting temperature; and ΔH^0_m is the heat of fusion per unit mass.

Equations (4)–(7) are used for crystallization occurring in regimes I and III. From eq. (6), the plot of $1/n$ ln $K + U^*/(R(T_c - T_\infty))$ against $(fT_c\Delta T)^{-1}$ is a straight line whose slope gives the value of K_g (Fig. 4), so the values of σ_e can be defined from formal eq. (7), and the following stand values were employed[24]:

$U^* = 6270$ J/mol, $T_\infty = T_g - 30 = 239.6$ K, $T^0_m = 481$ K, $f = 2T_c/(T^0_m + T_c)$, $b_0 = 6056 \times 10^{-10}$ m, $\sigma = 8.79 \times 10^{-3}$ J/m^2, $H^0_m = 134$ J/cm^3, $K_b = 1.35 \times 10^{-16}$ J/(mol K).

The values of K_g and σ_e are calculated from Figure 4 and listed in Table III.

As shown, for PP/Nu-(K + Na)/LDPE (100/0/0), (100/0/3), (100/0.3/0), and (100/0.3/3), the fold surface energy is 0.188, 0.167, 0.159, and 0.131 J/m^2, respectively. Feng et al.[8] studied the kinetics of DBS on PP crystallization, and found that fold surface energy, σ_e, decreased in nucleated PP also. Obviously, the addition of Nu-(K + Na), LDPE, or both, could decrease the fold surface energy of PP blends, and the rate of crystal nucleation are increased markedly. Especially, 0.3% Nu-(K + Na) cooperating with 3% LDPE shows the most efficient nucleating ability.

It is well known that the overall crystallization rate of polymers is determined by both the rate of crystal nucleation and the rate of crystal growth. When nucleating agents are added into polymers, some of them will become the crystalline nuclei, from which the crystals start developing. The spherulite will continue

growing until it impinges on another spherulite and then stops augmentation. The σ_e of PP/Nu-(K + Na)/ LDPE (100/0.3/3) is the lowest among the PP blends, it has the fastest rate of crystal nucleation, a larger number of nuclei should be produced in PP/Nu-(K + Na)/LDPE (100/0.3/3) ternary blends, and more spherulites would be formed in PP/Nu-(K + Na)/ LDPE ternary blends during crystallization, but they did not grow large enough to overlap. So, the size of spherulites in ternary blends should be the smallest among the PP blends, and PP/Nu-(K + Na)/LDPE (100/0.3/3) ternary blends exhibited the best transparency.

Spherulitic morphologies of PP samples

The PLM photographs of PP samples are showed in Figure 5. For pure PP, as could be seen in Figure 5, the average diameter of spherulites is 200 μm and the spherulite interfaces are very clear. Addition of only 3% LDPE reduces the spherulites size to 100 μm evidently, but the interfaces are still easy to be discerned. When 0.3% Nu-(K + Na) was added, the spherulites size of PP is decreased to 50 μm, because Nu-(K + Na) was a good nucleating agent for PP. When LDPE and Nu-(K + Na) were added to PP at the same time, the spherulites became further smaller and the boundaries became rough in the whole fields. This also proves that Nu-(K + Na) produced more heterogeneous nuclei in PP/Nu-(K + Na)/LDPE ternary blends during crystallization. Thus, the light scattering on the interface of spherulites were reduced markedly, and the transparency of PP was increased obviously.

Compatibility of PP samples

DMA is performed for the blends to obtain information on molecular chain motions and mechanical properties. Identification of the glass transition temperature (T_g) is one of the most common uses of DMA and generally T_g is related to the motion of the main chain and the relaxation of segments.[25]

Figure 6 shows the tanδ versus temperature curves for PP/Nu-(K + Na)/LDPE blends of different compositions. As could be seen, the T_g of pure PP is 14°C. The crystalline polymers have multiple transitions arising from relaxations associated with the amor-

TABLE III
Values of K_g and σ_e

PP/Nu-(K + Na)/LDPE	K_g ($\times 10^6$k^2)	σ_e (J/m^2)
100/0/0	1.15	0.188
100/0/3	1.03	0.167
100/0.3/0	0.98	0.159
100/0.3/3	0.81	0.131

PP/Nu-(K+Na)/LDPE=100/0/0

PP/Nu-(K+Na)/LDPE=100/0/3

PP/Nu-(K+Na)/LDPE=100/0.3/0
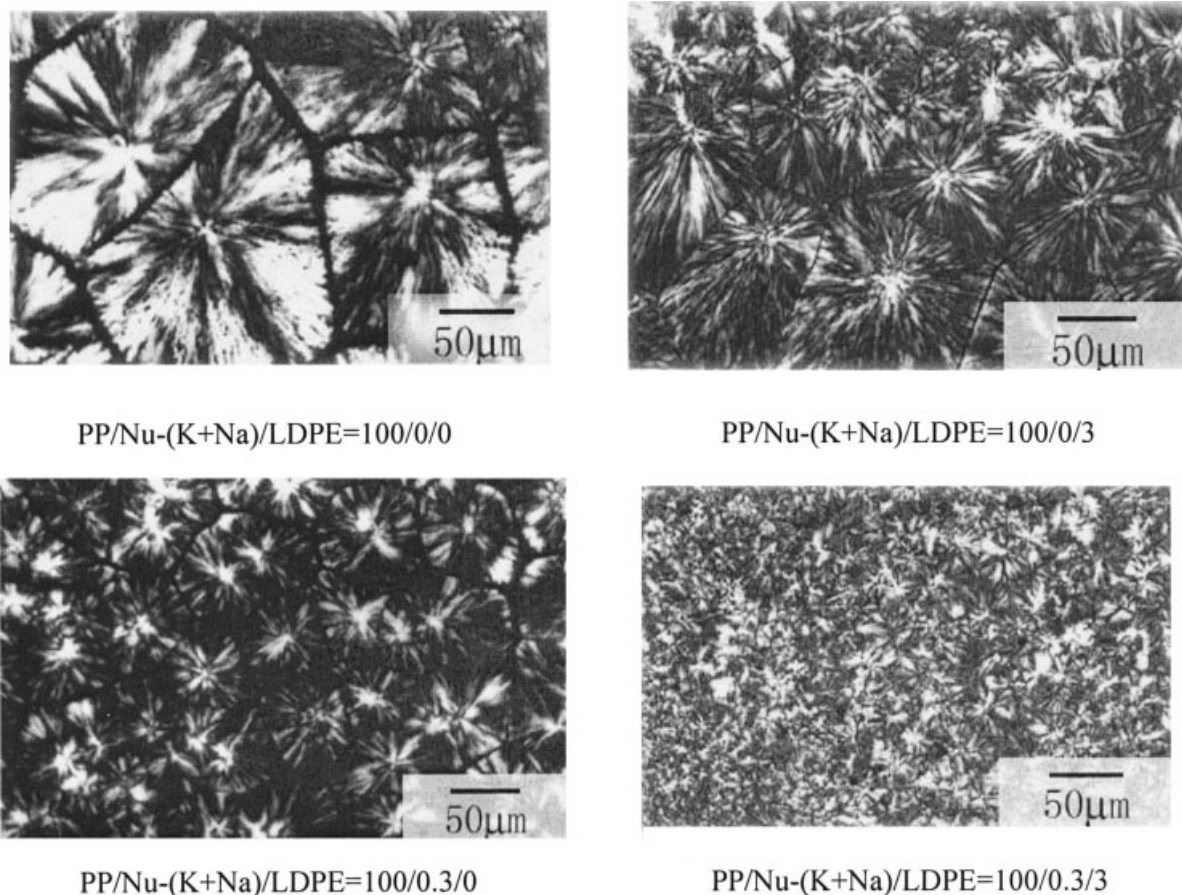
PP/Nu-(K+Na)/LDPE=100/0.3/3

Figure 5 PLM micrographs of PP/Nu-(K + Na)/LDPE blends.

phous phase, the crystalline phase, or both. More often, the β-transitions is considered as T_g of PE than the γ-transitions. The T_g of LDPE is in the temperature regions of approximately $-10°C$.[26–28] The γ-transi-

Figure 6 The tanδ *versus* temperature for PP/Nu-(K + Na)/LDPE blends.

tions of LDPE in Figure 6 is in the temperature regions of approximately $-130°C$, but the β-transitions is hardly detectable in Figure 6. When 3% LDPE is added to PP, the T_g of PP is reduced to 9°C, which indicated that the T_g of PP shifted to the T_g of LDPE, and that PP and LDPE have part compatibility with this content of LDPE. When 0.3% Nu-(K + Na) and 3% LDPE were added, the T_g of PP shifted to lower temperature and the relaxation peak of PP became broader. This indicates that the compatibility of PP and LDPE was further improved by Nu-(K + Na), *i.e.*, Nu-(K + Na) acted as a nucleating agent as well as a compatibilizer in the blends.

The scanning electron microscope micrographs of the morphologies of PP blend fracture surfaces are presented in Figure 7. Introducing 3% LDPE to PP, LDPE particles with about 0.3 μm (300 nm) in size are observed clearly within a continuous matrix of PP, though there was a little compatibility in the blend. With the addition of 0.3% Nu-(K + Na) in PP, no noticeable change appears compared with that of pure PP. When 3% LDPE and 0.3% Nu-(K + Na) were added to PP at the same time, LDPE particles could not be observed directly, this also proves that
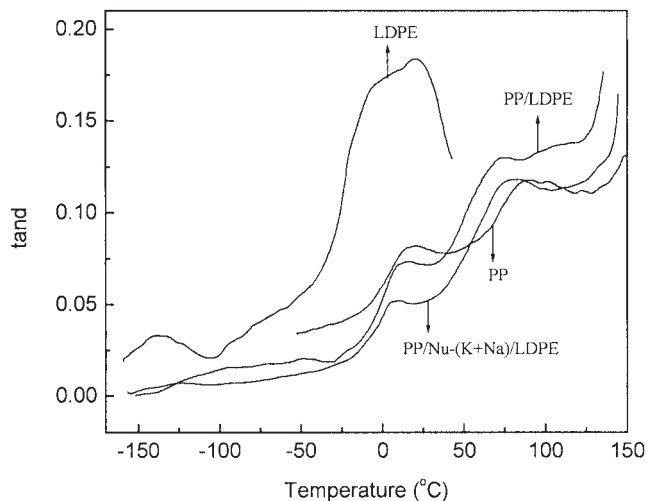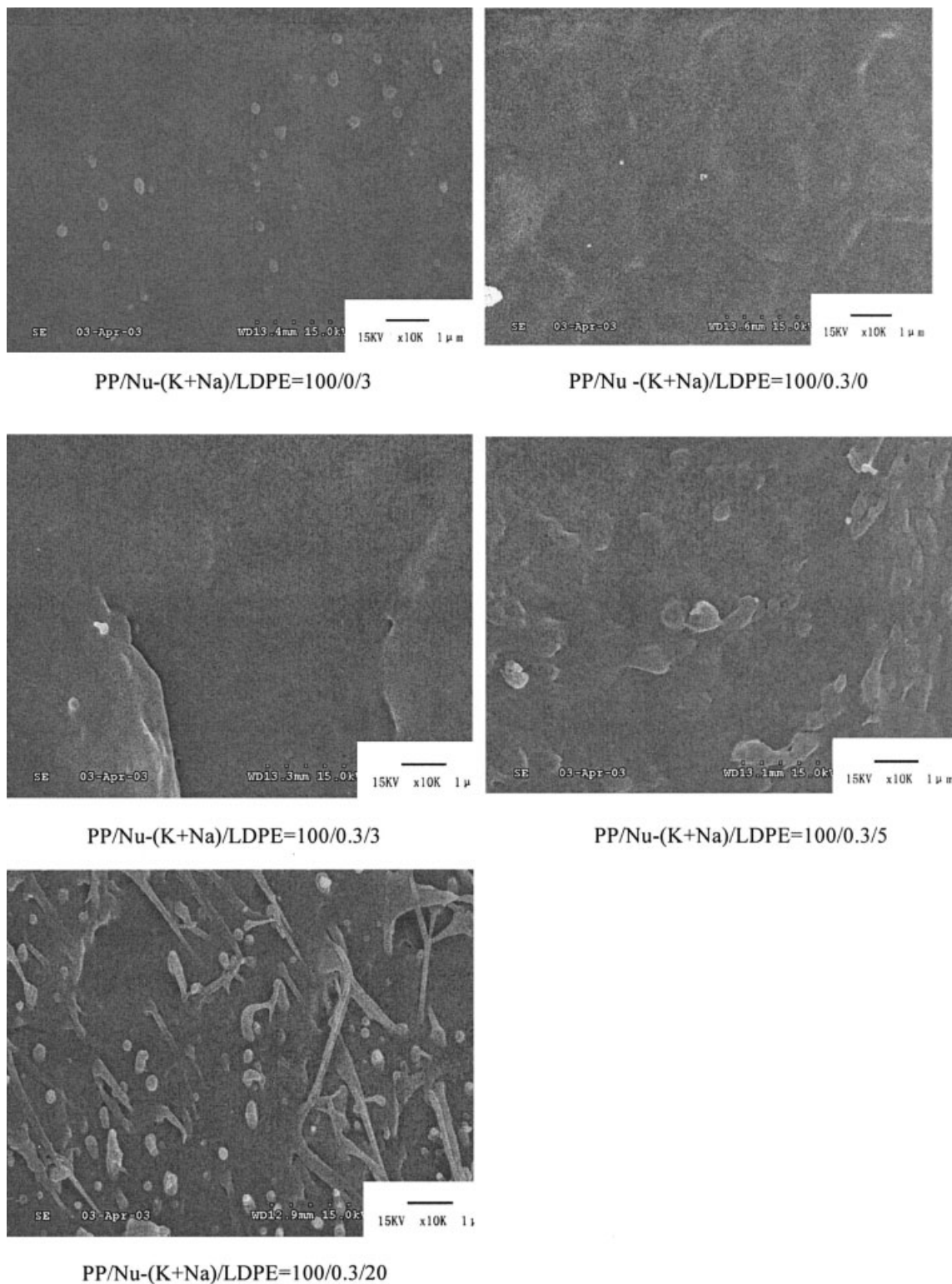
Figure 7 SEM micrographs of PP/Nu-(K + Na)/LDPE blends.

Nu-(K + Na) improved the compatibility of PP and LDPE, and the LDPE was dispersed in PP more uniformly. In fact, we do not expect the blend to be a truly homogeneous or a single state, but a state with particles sizes below the critical size for light scattering.[29] Under this condition, the light scattering originating from the decrease of LDPE disperse phase would be reduced to great extent. So the transparency of this ternary blend was improved remarkably.

However, the compatible range of the PP and the LDPE was limited. As shown in Figure 7, with the content of LDPE increasing, the PP blend fracture surfaces morphologies had changed markedly. When 5% LDPE was added to PP, the LDPE disperse phase with the average size of 0.5 μm is easy to be observed. The reason may be that the more addition of LDPE was not compatible with PP any more, and the excess fractions except 3% became a disperse phase in the blend. When 20% LDPE was added to PP, the size and number of disperse phase increased greatly, the light was scattered severely on the interface of two phases, and so the transparency of PP was reduced gradually.

CONCLUSIONS

The rosin-type clarifying agent Nu-(K + Na) substantially improves the transparency and crystallization temperatures of PP and decreases the size of spherulites also. When a small amount of LDPE (3%) was added to PP, the nucleating efficiency of Nu-(K + Na) was further improved. Thus, the crystallization rate of PP increased greatly, the spherulites of PP became much smaller and dispersed more uniformly, and the transparency of PP was improved evidently. Kinetics analysis of PP isothermal crystallization proves that Nu-(K + Na) decreases the fold surface energy and promotes the nucleation and crystallization of PP. With the cooperation of LDPE and Nu-(K + Na) in PP, the chain fold free energy of PP was further decreased substantially, and a larger number of nuclei should be produced in PP/Nu-(K + Na)/LDPE (100/0.3/3) ternary blends during crystallization; thus, the crystallization rate were increased markedly.

The DMA and SEM results proves that Nu-(K + Na) improved the compatibility of PP and LDPE, and the LDPE was dispersed in PP more uniformly. Thus, the light scattering originating from the LDPE disperse phase was reduced to great extent, and this was also of benefit to the transparency of PP.

References

1. Hideki, S.; Mikio, N.; Tetsuji, K.; Kimio, U.; Masao, M.; Yukiharu, Y.; Hiroyuki, H.; Junji, T.; Kan, M. Eur. Pat. 686,663 (1995).
2. Kazumasa, F.; Hitoshi, I. Eur. Pat. 785,231 (1997).
3. Takao, T.; Takeshi, O.; Shigenobu, K.; Tatsuo, K. Jpn. Kokai Tokkyo Koho 10,251,463 (1998).
4. Zhu, G.; Li, C.; Li, Z. Eur Polym J 2001, 37, 1007.
5. Li, C.; Zhu, G.; Li, Z. J Appl Polym Sci 2002, 83, 1069.
6. Li, C.; Zhang, D.; Li, Z. J Appl Polym Sci 2002, 85, 2644.
7. Li, C.; Li, W.; Wang, H.; Zhang, D.; Li, Z. J Appl Polym Sci 2003, 88, 2804.
8. Feng, Y.; Jin, X.; Hay, J. N. J Appl Polym Sci 1997, 69, 2089.
9. Wang, H.; Li, C.; Zhang, D.; Li, Z. J Appl Polym Sci 2003, 89, 2137.
10. Tammy, L. S.; Divakaran, M.; Long, K. B.; Yash, P. K.; Robert, G. B.; Willis, B. H.; Sean, C.; John, J. J.; Shari, B. Macromolecule 1994, 27, 3147.
11. Avalos, F.; Lopez-Manchado, M. A.; Arroyo, M. Polymer 1996, 37, 5681.
12. Li, J.; Shanks, R. A.; Honey, R.; Greenway, G. R. Polymer 2001, 42, 7685.
13. Shanks, R. A.; Li, J.; Yu, L. Polymer 2000, 41, 2133.
14. Li, J.; Shanks, R. A.; Long, Y. Polymer 2001, 42, 1941.
15. Tselios, Ch.; Biliaris, D.; Maslis, V.; Panayiotou, C. Polymer 1998, 39, 6807.
16. Halbrook, N. J.; Lawrence, R. V. J Org Chem 1966, 31, 4246.
17. Avrami, M. J Chem Phys 1940, 8, 212.
18. Menczel, J.; Varga, J. J Therm Anal 1983, 28, 161.
19. Fujiyama, M.; Wakino, T. J Appl Polym Sci 1991, 42, 2739.
20. Binsbergen, F. L. J Macromol Sci Phys 1970, 4, 837.
21. Hoffman, J. D. Soc Plast Eng Trans 1960, 4, 315.
22. Hoffman, J. D. Polymer 1983, 24, 3.
23. Alfonso, G. C.; Chiappa, V.; Liu, J.; Sadiku, E. R. Eur Polym J 1991, 27, 795.
24. Hoffman, J. D.; Frolen, L. J.; Ross, G. S.; Lauritzen, J. I. J Res Natl Bur Stand Sect A 1975, 79, 671.
25. Hippi, U.; Mattila, J.; Korhonen, M.; Seppala, J. Polymer 2003, 44, 1193.
26. Khanna, Y. P.; Turi, E. A.; Taylor T. J.; Vickroy, V. V.; Abbott, R. F. Macromolecules 1985, 18, 1302.
27. Boyd, R. H. Polymer 1985, 26, 323.
28. Boyd, R. H. Polymer 1985, 26, 1123.
29. Stachurski, Z. H.; Edward, G. H.; Yin, M.; Long, Y. Macromolecule 1996, 29, 2131.